Air Quality, Atmosphere & Health
https://doi.org/10.1007/s11869-022-01179-y

Temporal and spatial distribution mapping of particulate matter in southwest of Iran using remote sensing, GIS, and statistical techniques

Arezoo Soleimany[1] · Eisa Solgi[1] · Khosro Ashrafi[2] · Reza Jafari[3] · Raimondas Grubliauskas[4]

Received: 18 September 2021 / Accepted: 3 March 2022
© The Author(s), under exclusive licence to Springer Nature B.V. 2022

Abstract

Major items concerning air and weather researches include the amount of aerosols and particulate matter (PM) present in the air. Satellite-retrieved, aerosol optical depth (AOD) is a widely used method for the mapping of particulate matter (PM_{10}) concentrations. Precise estimate and mapping of PM_{10} depend on the resolution of AOD data and the mathematical model, which considers the spatially non-stationary relationship between PM_{10} and AOD. Khuzestan province of Iran is deficient in a powerful and validated resolved model of PM_{10} with high spatial temporal resolution. Therefore, the purpose of this study is to investigate and monitor the concentration of PM_{10} in 26 air quality monitoring stations along with meteorological data obtained from 21 synoptic stations, aerosol optical depth (AOD) extracted MODIS Terra/Aqua, and their relationship which were analyzed using GIS services, statistical models, and remote sensing throughout Khuzestan province of Iran from January 2008 to December 2018. This research verified the MCD19A2 AOD product and then proved that MCD19A2 could accurately indicate the aerosol distribution in the Khuzestan province of Iran. Analysis of average annual MCD19A2 AOD data revealed 2008 and 2009 as the most polluted years in Khuzestan province during 11 years (2008–2018) of study. The study of dust trends showed a significant increase in spring and summer in the study area. The results of this study indicated that PM_{10} is influenced by AOD and meteorological parameters. Meteorological data together with simplified aerosol retrieval algorithm-retrieved AOD at 1-km resolution were applied as the predictors for the linear regression (LR), multiple linear regression (MLR), the ordinary least squares (OLS), and geographically weighted regression (GWR) models to predict the spatial distribution of PM_{10} concentrations. Among all the statistical models, the GWR performed better and had higher accuracy. Also, the investigation of indicators such as root mean squared errors (RMSE), mean absolute error (MAE), Akaike's information criterion (AICc), adjusted coefficient of determination (R^2), normal (Z) scores, and Moran's I of the model residuals, to evaluate the accuracy of the studied models, showed high accuracy and excellent performance of the GWR model in predicting the amount of particulate matter in the study area. These results suggested that the GWR model could provide a reliable way to predict the spatial distribution of PM_{10} concentrations over Khuzestan province. Assessment of short- and long-term human exposures and then investigation of the effects of particulate matter will be possible through our model.

Keywords Particulate matter (PM_{10}) · Aerosol optical depth (AOD) · Khuzestan province · Geographically weighted regression (GWR) · Ordinary least squares (OLS)

Introduction

Dust storms, as the most common phenomenon in many parts of the world, notably in the arid and semi-arid regions, are a severe threat to human societies. The atmospheric aerosol distribution must be tracked to find the effect of aerosols on air quality and its consequent impact on human health in a region (Pope et al. 2002; Liu et al. 2011). One of the pollutants which may cause humans to have respiratory problems is PM_{10} (Balakrishnan et al. 2002; Pope et al. 2011a, b; Ha Trang and Tripathi 2014; Kamarul Zaman et al. 2017). Moreover, exposure to PM_{10}, and PMs finer than 2.5 μm ($PM_{2.5}$), is shown to increase the risk of cardiovascular diseases (Dominici et al. 2006), abnormalities at birth, and early death (Ballester et al. 2010). PM_{10} may influence

✉ Eisa Solgi
e.solgi@yahoo.com

Extended author information available on the last page of the article

Published online: 23 March 2022

the weather and climate system by disturbing normal solar radiation leading to warming and/or cooling (Ramanathan and Carmichael 2008). The changes depend on the particle type (i.e., dust, soot, or anthropogenic pollution) and their optical and chemical characteristics. It is more concerning in developing countries since the maximum allowable particles determined by the World Health Organization are often exceeded.

Most studies conducted on the quality of air, precipitation, and climate radiation focus on aerosols and particulate matter as the main factors. The primary pollutants which should be regularly and carefully observed by the Environmental Protection Agencies are PM_{10} and $PM_{2.5}$ (PM with diameter < 10 μm and 2.5 μm, respectively) (Han et al. 2015). The measurement of PM is an essential part of studying air quality, public health, and epidemiology. It plays critical lore in making decisions for short-term and long-term policies and implementations. Aerosols in the air can absorb and scatter the solar radiation resulting in attenuated radiation reaching the earth's surface (Haywood and Ramaswamy 1998; Hatzianastassiou et al. 2007; Misra et al. 2015; Pawar et al. 2015; Kolhe et al. 2016). Thus, aerosols and pollutants in the air can, directly and indirectly, affect the radiative energy budget of the earth-atmosphere system and consequently alter the earth's climate (Papadimas et al. 2008; Pawar et al. 2015; Kolhe et al. 2016; Ali et al. 2017).

Assessment of particulate matter is usually performed from various ground monitoring stations. However, such measures are limited to points that cannot provide the complete spatial coverage required for mapping regional air quality and assessment of human exposure pollutants (Tian and Chen 2010). Modeling of air quality is an alternate way for air quality and particulate matter spatial distribution assessment, which needs some information about chemical and physical processes in the atmosphere as well as a comprehensive list of data about the emissions as an input (Koelemeijer et al. 2006). Even though ground-based measurements are more precise than satellite ones, aerosol optical depth (AOD) retrieved from satellite sensors has been discussed as a good representative for ground-observed particulate matter mass concentrations and a great tool to monitor aerosol pollution (Koelemeijer et al. 2006; Al-Saadi et al. 2005; Engel-Cox et al. 2004; Chu et al. 2003). The Moderate Resolution Imaging Spectroradiometer (MODIS) gives the distribution of AOD globally daily at a spatial resolution of 10×10 km^2 which covers ocean and land (Grgurić et al. 2014).

Recently, many studies have utilized satellite measurements of AOD, where it has been called aerosol optical thickness, to help predict particulate matter concentrations over different regions or during various times (Stafoggia et al. 2019, 2016; de Hoogh et al. 2018; Di et al. 2016; Kloog et al. 2012; Lee et al. 2015). Monitoring AOD via satellite remote sensing methods gives an alternative means for the particulate matter concentration measurement at the ground level by modeling the relationships between AOD and PM (Ali et al. 2021). During the last 10 years, many studies have utilized satellite remote sensing as a powerful and economical means of estimating PM levels from the retrieved parameter of AOD. Aerosol optical depth data, representing particulate matter concentrations in the atmosphere, are non-dimensional parameters computed by integrating light scattering of aerosols from ground surface up to the top of the atmosphere (Liou (2002), Dinoi et al. (2010), Hu et al. (2014), Seo et al. (2015), Ghotbi et al. (2016)). The newly released MCD19A2 product integrates Terra and Aqua along with utilizing the multi-angle implementation of the atmospheric correction (MAIAC) algorithm (Lyapustin et al. 2018; Karagulian et al. 2019).

Numerous results in most studies related to the relationship between AOD extracted from MODIS images and the concentration of particulate matter for different regions and periods indicate a linear relationship between them and also show the positive effect of AOD in predicting the concentration of particulate matter. Several statistical models involving spatial and/or temporal heterogeneities have been developed during the recent 20 years. Geographically weighted regression (GWR) is a technique that was designed for extending the traditional global model fitted by ordinary least squares (OLS). It could successfully manage model errors such as spatial heterogeneity and autocorrelation (Fotheringham et al. 2002; Zhang et al. 2005, 2009; Wei et al. 2019). GWR is a part of local modeling techniques which fits a regression model for each geographic location considering the neighbors within a specific bandwidth and distance-dependent weight function (Wei et al. 2019).

Broomandi et al. (2018) reported that dust particles arrive in the Ahvaz City (capital of Khuzestan province) from the north-western and central parts of Iraq and eastern parts of Syria. Central Iraq was also reported to be one of the primary dust sources of Ahvaz by Noroozi and Shoaei (2018). Additionally, Azizi et al. (2012) studied dust sources for Western Iran and introduced the regions around the border between Iraq and Syria as the primary source. The United Nations Environment Program has announced some factors as exacerbating dust events. The factors include the occurrence of droughts in South-west Iran and Iraq as an adjacent country, reduced surface and subsurface soil moisture level, decrease in vegetation cover, and the development of sedimentary and fine-grained areas (Environment in Iraq: UNEP Progress Report 2003; Javadian et al. 2019). In recent years, Iran and especially the south-western provinces, including Khuzestan province, have witnessed a significant increase in the occurrence of dust. With the rise in the event of dust storms in recent years in south-western Iran and especially in Khuzestan province and consequently the reduction of

air quality in these areas, the study of this phenomenon is of great importance. There has not been a powerful validated high-resolution spatial-temporally resolved model of PM for the Khuzestan province of Iran. Therefore, in this research, this strategic and specific province has been selected as a study area. Due to the importance of PM_{10} pollutants on health and the effects mentioned earlier, our study area, in addition to having internal dust centers, sees dust coming from neighboring countries such as Iraq, Saudi Arabia, Syria, and Kuwait; these pollutants are high in this area. According to these reasons, the target contaminant was selected in this study.

The purpose of this study is to investigate and monitor the concentration of particulate matter in 26 air quality monitoring stations throughout Khuzestan province of Iran along with meteorological data, aerosol optical depth, and their relationship using GIS services, statistical models, and remote sensing from January 2008 to December 2018. We utilized aerosol ground observation data, including air monitoring stations, to verify different aerosol products over Khuzestan province. In this research, via remote sensing techniques, we aim to verify MCD19A2 AOD and investigate the correlation between AOD and particulate matter (PM_{10}) concentration in Khuzestan province. Also, the present study implemented four models, namely linear model (LM), multiple linear regression (MLR), and ordinary least square regression (OLS) as the benchmark for comparing models, traditional geographically weighted regression (GWR), for the estimation of PM_{10} over the Khuzestan area, Iran, based on satellite-derived AOD and other related parameters, such as surface temperature, relative humidity, wind speed, and precipitation. The goodness of fit, prediction accuracy, uncertainty and accuracy of models, and model residuals were determined and compared according to modified Akaike's information criterion (AICc), adjusted coefficient of determination (R^2 a), root mean-squared errors (RMSE), mean absolute error (MAE), normal (Z) scores, and Moran's I of the model residuals.

Methodology

Study area

Khuzestan province in south-western of Iran is located between 29° 57′–33° 00′ N latitude and 47° 40′–50° 33′ E longitude with an area of about 64,055 km^2 and has a population of 4,711,000. Iraq from the west, the Persian Gulf from the south and provinces including Chahar Mahal and Bakhtiari, Kohgiluyeh and Boyer Ahmad from the northeast and east, Lorestan from the north, and Bushehr from the southeast border of Khuzestan province. This province is adjacent to Iraq, but the waves of westerly winds that are the prevailing phenomenon in the region also pass through Syria, northern Saudi Arabia, and Kuwait on their way to Khuzestan. In addition, a large area of Khuzestan province is also covered by active desert centers. This, in turn, creates dust storms on a local scale. For this reason, due to the occurrence of drought in recent years, this province has a higher incidence of dust than other provinces in the country, and many problems due to reduced air quality have been observed due to the establishment of dust masses in the province. Therefore, in this study, Khuzestan province was selected as the study area (Fig. 1) and was evaluated from 2008 to 2018.

Data and process

Collection and processing of air monitoring stations data

We obtained hourly concentrations of PM_{10} data for the 11 years of 2008–2018 from 26 air quality monitoring stations in Khuzestan province. To analyze the pollutants spatiotemporally, concentrations of each particulate matter (PM_{10}) measured every hour were sorted as daily, monthly, and annual (Faridi et al. 2018; Wu et al. 2018). The mean yearly concentration got utilized for the prediction of the concentration data (Wu et al. 2018). Figure 1 indicates the location of air quality monitoring stations in the Khuzestan province.

Collection and processing time series of meteorological parameters

Meteorological parameters such as relative humidity, wind speed, and temperature strongly affect the concentration of particulate matter (PM). Increasing the temperature increases the photochemical reactions resulting in the production of particulate matter (PM) in the atmosphere. Also, the phenomenon of temperature inversion and atmospheric stability on cold days of the year causes the accumulation and increase of PM pollutants concentration. High relative humidity increases and produces secondary pollutants that can change the size and optical properties of particulate matter (PM) and changes in light scattering by these particles, which affects the optical depth of the pollutant recorded by the sensor.

In this study, temporal changes in meteorological parameters such as temperature, wind speed, sum-precipitation, humidity, and visibility during a 30-year statistical period have been investigated. But, to analyze and monitor the relationship between the data of suspended particles concentration and overlap with them, the results of 11 years of analysis of them are given in the results section. The meteorological data were provided by the Iranian Meteorological Organization (http://www.irimo.ir) for 21 synoptic stations

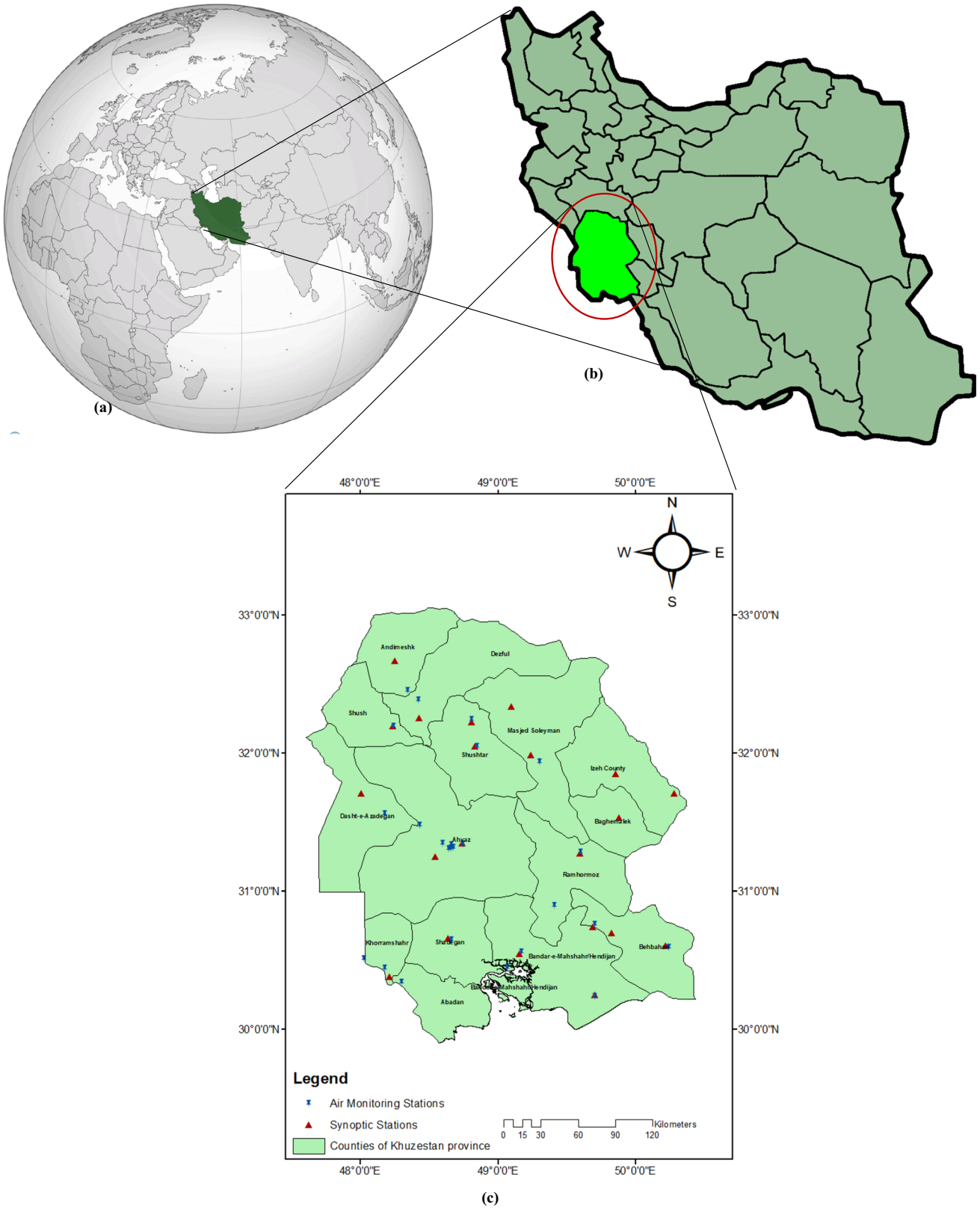


Fig. 1 **a** Location of Iran country on the world. **b** Location of Khuzestan province on the Iran country. **c** Study area and location of air quality monitoring stations and synoptic stations in Khuzestan province

from 1988 to 2018. The location of synoptic stations of Khuzestan province is shown in Fig. 1.

MODIS AOD data and pre-processing

Aerosol optical depth (AOD) is a parameter obtained from a satellite that measures the degree to which particles floating in the air affect the light radiation by absorption or scattering. Hence, it can be regarded as an indirect scale for the particles in the column of air at a particular time (Lyapustin et al. 2018; Stafoggia et al. 2019). In the present study, we used the MCD19A2 Version 6 data product from 2008 to December 2018. This product is a Moderate Resolution Imaging Spectroradiometer (MODIS) Terra and Aqua Combined Multi-Angle Implementation of Atmospheric Correction (MAIAC) Land Aerosol Optical Depth (AOD) gridded Level 2 product made daily at 1-km pixel resolution (Lyapustin et al. 2018; Karagulian et al. 2019). The MAIAC product, developed for MODIS's data processing, is a novel advanced product that employs time series analysis together with a combination of pixel-based and image-based processing to improve cloud detection accuracy, aerosol retrieval, and atmospheric correction (Wang et al. 2021). The MCD19A2 product gives the atmospheric characteristics and view geometry used to compute the MAIAC Land Surface Bidirectional Reflectance Factor (BRF) or surface reflectance, MCD19A1 product.

Google Earth Engine (GEE) is a cloud computing platform launched by Google in 2010. GEE uses Google's computational infrastructure and available open-access RS datasets (Amani et al. 2020; Soleimany et al. 2021; Gorelick et al. 2017). GEE is the most known and largest geodata processing platform, which helps the scientific discovery process by presenting users access to many remotely sensed datasets for free (Amani et al. 2020). Access to GEE can be gained via an Internet-based Application Programming Interface (API) and a Web-based Interactive Development Environment (Amani et al. 2020; Gorelick et al. 2017). Moreover, users with no expertise in Web programming or HyperText Markup Language can use GEE for various applications (Amani et al. 2020; Gorelick et al. 2017). Different features of GEE include automatic parallel processing and being a fast computational platform for dealing with the challenges of big data processing (Amani et al. 2020; Gorelick et al. 2017; Hird et al. 2017; Ali et al. 2020). In this study, the datasets were obtained from and processed by the GEE API.

Statistical analyses

In different problems, there are several methods to estimate a parameter through one or more other variables, which is one of the standard methods to predict the behavior of a dependent variable through independent variables of a linear regression model (Eq. 1). All the analyses were performed individually for each year, from 2008 to 2018. To extract AOD data from buffers with a radius of 2-km air quality monitoring stations.

$$PM_{10i} = \beta_0 + \beta_1(AOD) \tag{1}$$

The next model used in this research is multiple linear regression. The multiple linear regression (MLR) determines significant variables and eliminates collinearities among them. MLR has been employed to predict PM from satellite AOD for many years. MLR is known as the most prevalent form of linear regression analysis (Xiao et al. 2018). Multiple linear regression is an analysis technique that describes the relationship between one continuous dependent variable and two or more independent variables to predict a response. In other words, in this method, all variables are entered in order of minimum tolerance (tolerance statistic) to analyze the impact of independent variables on the dependent variable. A computed VIF and a tolerance value are given to each independent variable. With large VIF values (>10, for instance) and small tolerance, i.e., <0.1, significant collinearity is concluded, which needs correction and elimination of the offending variables from the model (Xiao et al. 2018).

We chose PM_{10} obtained from ground level as the dependent variable and AOD as the independent. Also, temperature, humidity, wind speed, and precipitation were considered in the model as covariates too (Chu et al. 2017). Equation 2 represents the multiple regression model.

$$PM_{10i} = \beta_0 + \beta_1(AOD) + \beta_2(T) + \beta_3(RH) + \beta_4(WS) + \beta_5(P) \tag{2}$$

In Eq. 2, $PM_{10}i$ represents the concentration of particulate matter in station i and AOD, T, RH, WS, P, and β_0 to β_5 express aerosol optical depth, temperature, relative humidity, wind speed, precipitation, and regression coefficients, respectively.

The ordinary least squares regression (OLS) method is a statistical technique through which the unknown parameters of a linear regression model are estimated. The objective function, which represents the sum of squares of the differences between the experimental values and the model predicted values, is minimized using OLS (Xiao et al. 2018; Mokhtari et al. 2021). The objective function here is:

$$\varnothing = e_y^T Q_y^{-1} e_y \tag{3}$$

where e_y is the error matrix of the observation vector y. When the observation vector is $m \times 1$, the e_y matrix will also be $m \times 1$, and then Q_y is the $m \times m$ covariance matrix of observations (observations weight matrix). In the OLS model, a weight of 1 is equally allocated to each observation. The model considers the independent variables as

invariable and error-free observations and utilizes a simple and functional model (Eq. (4)). The unknown coefficients are obtained from the least-squares method according to the following Eq. (5):

$$y = X\beta + e_y \tag{4}$$

$$\hat{\beta} = \left(X^T X\right)^{-1} X^T y \tag{5}$$

In Eq. (5), T is the matrix transpose, $\left(X^T X\right)^{-1}$ is the inverse of the variance–covariance matrix, and X is the matrix of independent variables.

Fotheringham et al. (1998) developed an OLS-based method in which a local regression model was used to find the spatial heterogeneity. A geographically weighted regression (GWR) model considers spatial locations and uses the regional estimates of the parameters. The GWR model can show the impact of independent variables on dependent ones with the locations' variations and the spatial heterogeneity of the relationship among those variables. The unique characteristics of GWR helped us show the spatial variance of the relationship among PM_{10} concentrations, the annual average temperature (AAT), the annual average humidity (AAH), the annual average wind speed (AAWS), and the annual average sum-precipitation (AAP).

The global regression model is as follows:

$$y_i = \beta_0(u_i, v_i) + \sum_k \beta_k(u_i, v_i) x_{ik} + \varepsilon_i, \ (i = 1, 2, \ldots, n), \tag{6}$$

where (u_i, v_i) is the spatial coordinate of a specific point i and $\beta_k(u_i, v_i)$ is the regression coefficient of sample point i. ε_i is the random error of the independent distribution, usually assumed to be normally distributed if $\beta_k(u_1, v_1) = \beta_k(u_2, v_2) = \cdots \beta_k(u_n, v_n)$, then the model will be varied into an OLS model (Lin et al. 2015; Fotheringham et al. 2002).

Bandwidth, which is responsible for controlling the degree of smoothing, is an essential parameter for GWR. It can be found via two automatic methods: CV that minimizes a cross-validation (CV) function, and Akaike information criterion (AIC) that minimizes the AIC (Fotheringham et al., 2002). In this study, an adaptive kernel was chosen, which considered the spatial configuration of the features, and the bandwidth was obtained by minimizing the corrected Akaike information criterion value as it is less biased than AIC (Hurvich et al. 1998).

The spatial variance of the relationship between the PM_{10} concentrations and AOD and meteorological parameters (PM ~ AOD + Temp + RH + WS + Prec) in Khuzestan province was obtained through the following steps. PM is a function of and predictable by the following factors (as independent variables): the MODIS Terra/Aqua aerosol optical depth value AOD (unitless), Temp denotes temperature (°C), the relative humidity is RH (%), the WS is wind speed (m/s), and the sum precipitation is Prec (mm). To enhance the model's accuracy, among all variables, the significant independent ones were selected. First, Pearson's correlation coefficient was employed to find the variables with the strongest correlation to the independent variables. In the next step, evaluate the relationships between the PM concentrations, AOD, AAP, AAH, AAWS, and AAT based on MLR with data of Khuzestan province (Ma et al., 2013) in Iran for the period 2008–2018. Then, different combinations of the chosen variables were used to develop OLS-based models. The variables with p-values greater than 0.05 were ignored. Finally, the variables with the most potent effect on the R^2 were selected for developing the OLS and GWR models. The finalized GWR model is generally ascertained based on the model performance denoted by fitting the R^2 (highest) and the AICc (lowest) value.

All statistical analyses were carried out using the SPSS (version 26) and R statistical software, version 4.0.5. All maps were created with ArcGIS 10.4. Investigation and analysis of satellite products have been performed using JavaScript code in the Google Earth Engine platform.

Model evaluation

In this study, to compare the validity of the studied models, the coefficient of determination, the adjusted coefficient of determination (adjusted R-squared), the root mean square errors (RMSE), mean absolute error (MAE) (Noori et al. 2010; Mirzaei et al. 2019), and the corrected Akaike's information criterion (AICc) (Fotheringham et al. 2002), have been used.

Metrics are calculated using the following formulas:

$$RMSE = \sqrt{\frac{1}{n}\sum_{i=1}^{n}(y_j - \hat{y}_j)^2} \tag{7}$$

$$MAE = \frac{1}{n}\sum_{i=1}^{n}|y_j - \hat{y}_j| \tag{8}$$

where y_j and $\hat{y}_j$ refer to the observed and predicted values, respectively, and n indicates the number of data points.

$$AIC_C = AIC + \frac{2k(k+1)}{n-k-1} \tag{9}$$

$$AIC = 2k - 2\ln(\hat{L}) \tag{10}$$

K denotes the number of estimated parameters in the model, and $\hat{L}$ is the maximum value of the likelihood function for the model.

In this study, we also performed leave-one-station-out cross-validation to reflect the performance of the models used. In this study, using the leave-one-station-out

cross-validation (LOOCV) technique, observations of all stations except one station were used for training, and observation of the remaining stations was used to test the model. This process was repeated 26 times. At each stage, the observations (data) of a station were considered experimental data. The modeling accuracy was determined based on the average accuracy of all steps at the end of the process. Also, evaluation parameters such as RMSE and MAE calculated for this process were shown. The following figure shows the LOOCV technique (Fig. 2).

Results and discussion

Relationship between AOD with in situ *particulate matter (PM_{10})*

Figure 3 shows the linear relationship between the MCD19A2 AOD extracted from the MODIS Terra/Aqua satellite images and in situ measured PM_{10} concentration. As shown in the figure, a robust linear relationship was found between the MCD19A2 AOD product and PM_{10} measurements. The highest coefficient of determination (R^2) was observed in 2009 (Fig. 3). The results of verification indicated that MCD19A2 is highly accurate and reliable (Fig. 3). Thus, the MCD19A2 data can demonstrate the aerosol distribution in Khuzestan province accurately. The use of MCD19A2 for aerosol research and characterization in Khuzestan province is feasible and reliable.

Spatial distribution of AOD during 2008 to 2018

Statistical studies on the concentration of particulate matter (PM_{10}) in air quality monitoring stations in Khuzestan province showed that 2008 and 2009 is the peak and turning point of particulate matter and the frequency of dust storms, but in 2013 and 2014, a decreasing trend there is a noticeable amount of concentration of particulate matter and the frequency of dust. The spatial distribution of AOD at the study area level from 2008 to 2018 is shown in Fig. 4. As shown in this figure, the southern, southwestern, and central regions, which include Mahshahr, Hindijan, Abadan, Khorramshahr, Shadegan, Ahvaz, and Dasht-Azadegan, have given the highest AOD. Also, an 11-year study of the spatial distribution of AOD showed that the lowest values are related to the stations located in the north and northeast of the study area (Fig. 4). Analyses of annual average AOD data showed that 2008 and 2009 were the most polluted years in southwestern Iran. The findings of this study are consistent with the results of Javadian et al. (2019).

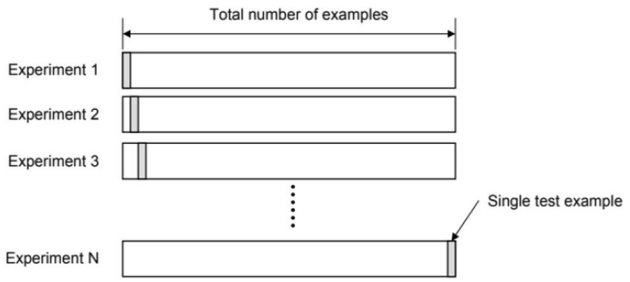


Fig.2 LOOCV technique

Monthly change trends in the daily mean MODIS MAIAC AOD

The highest amount of dust in the stations of the studied province is in April, May, June, and July (that is shown as red circles in Fig. 5). The lowest are in November and December based on environmental monitoring and satellite data. Being the hottest and driest months of the year, this result was expected in the region. It causes depletion of moisture from the soil and makes the environment susceptible to dust events. On the contrary, lower AOD is observed in winter when significant precipitations occur in the region and the surface soil is relatively moist (Javadian et al. 2019).

MODIS findings and air quality monitoring stations in the study area indicate that the monthly dust distribution has the highest concentration from April to August. Therefore, the intensity of dust until 2009 in the Middle East and summer and spring and its transfer to the west of the country has been confirmed in previous studies in the Middle East, which is affected by changes in climate parameters such as high wind speeds on the Red Sea and deserts. Changes in relative humidity, reduced rainfall, and reduced soil moisture, as well as changes in land use in the Middle East, have led to an intensification of dust activities. The study of dust trends showed a significant increase in spring and summer in the study area.

Also, examination of the daily distribution of aerosol optical depth during the study years showed that 2008, 2009, 2011, and 2012 had the highest levels of dust, which were similar to ground-based air quality monitoring stations in the study area (Fig. 5). Furthermore, Fig. 5 shows that AODs from 2015 to 2018 have increased compared to 2 years ago. This can be attributed to dramatically desiccation of water bodies in west Khuzestan and eastern parts of Iraq. These wetlands almost went dry in 2015 through 2018 and act as a dust source for dust storms in the area.

Iran is located in the arid and semiarid belt of the world and, on the other hand, the vicinity to the countries with poor vegetation cover, low precipitation, and high temperatures, such as Arabia, Iraq, and Syria, which are mostly the desert and are affected by desert conditions, air instability, and severe wind flow, is susceptible to dust storm phenomena. The alternating droughts in these areas have led to a

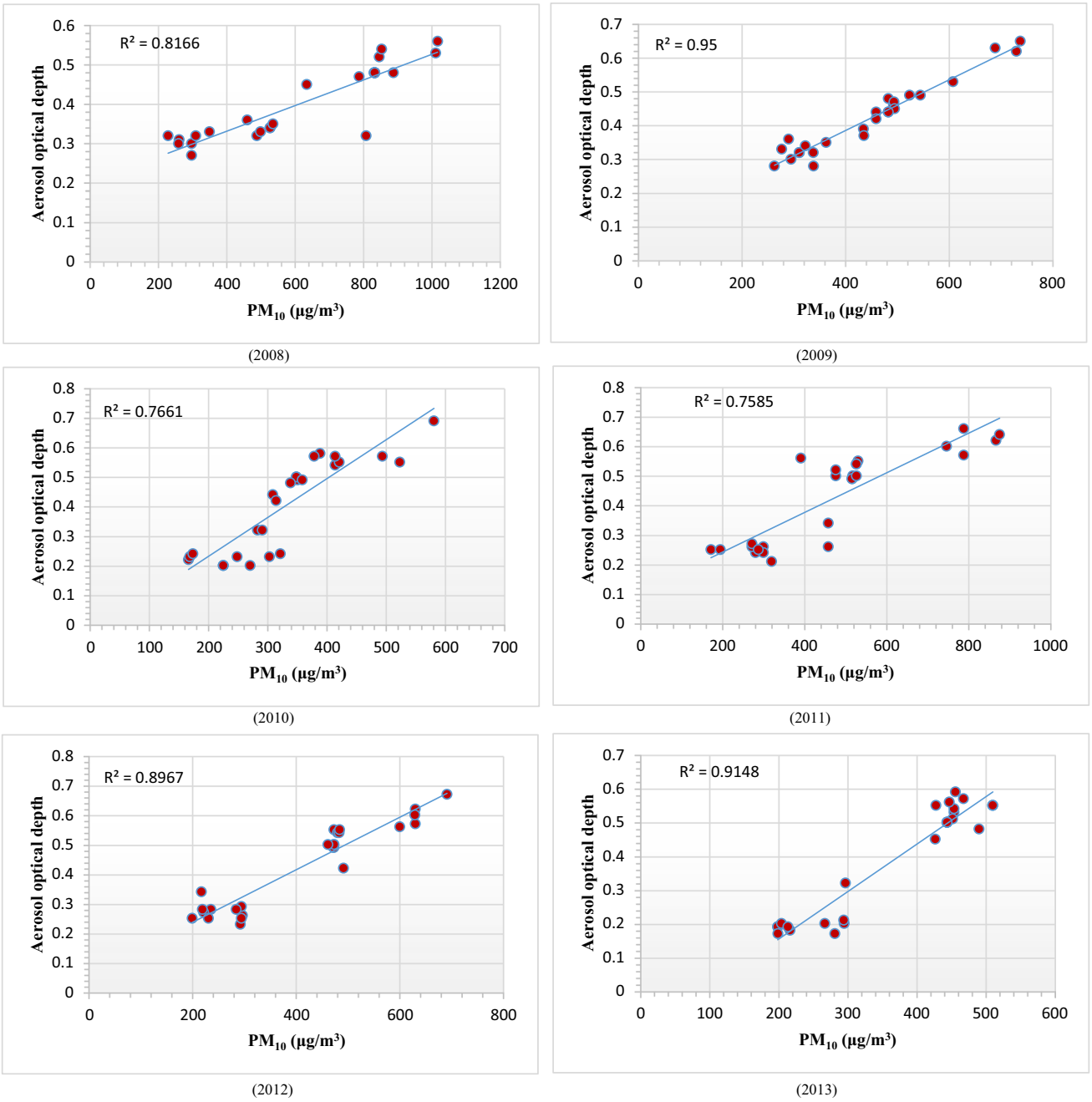
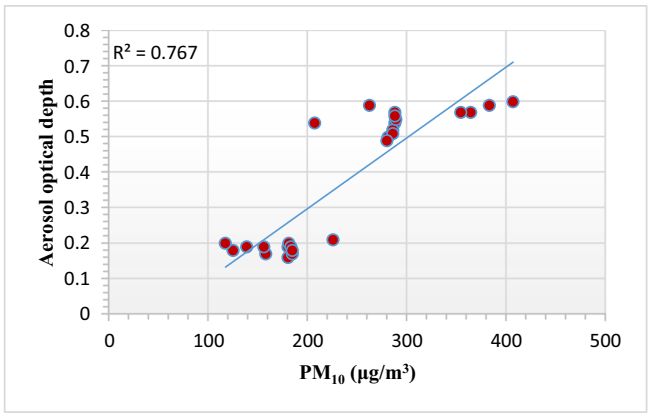


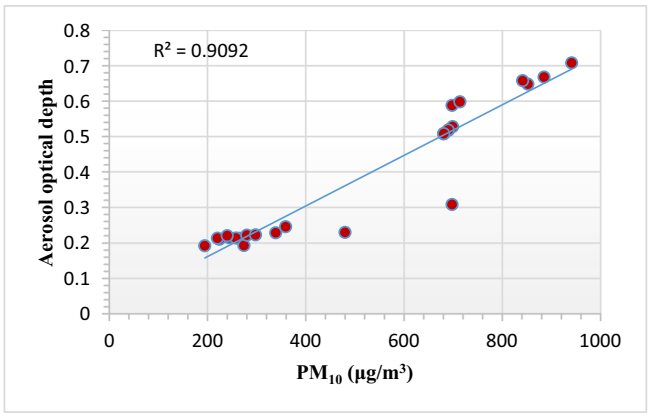
Fig. 3 Linear relation of MAIACA2 aerosol optical depth and in situ PM_{10} concentration from 2008 to 2018 during stations overall Khuzestan province of Iran

periodic dust phenomenon in the western parts of Iran. In addition, adverse use of natural resources and the environment by the people inside Iran and neighboring countries has worsened the event (Abdollahi et al. 2021). The role of two seasons, summer and spring, has been very colorful in the dust.

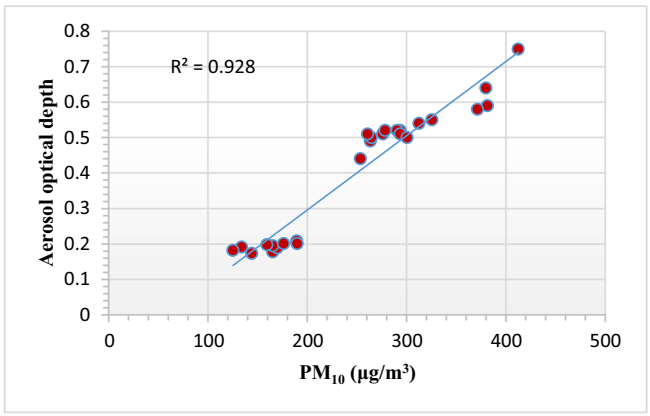
Both the monthly graphs obtained from the average hourly and daily concentrations of the AOD values



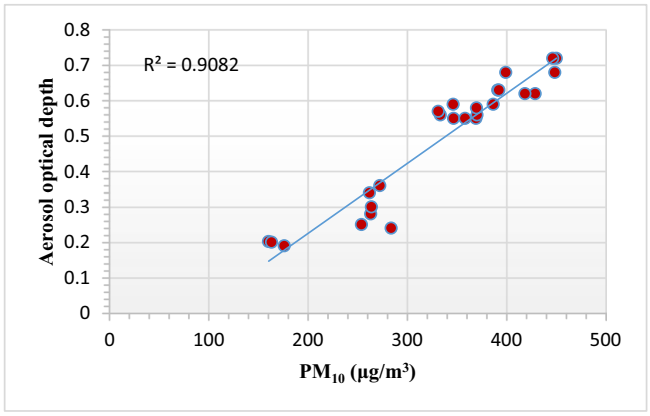
(2014)



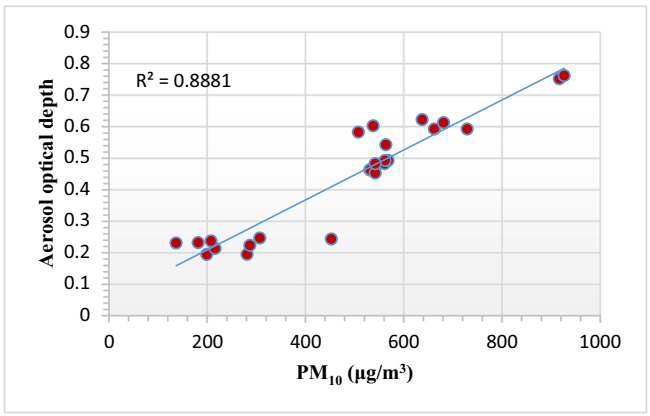
(2015)



(2016)



(2017)



(2018)

Fig. 3 (continued)

extracted from the satellite images and the investigating of the particulate matter (PM) air quality monitoring stations showed that in April, May, June, and July, as well as spring and summer seasons. We see the highest values of AOD and PM_{10}. According to the observational results, it can be said that in the study area of 2008 and 2009, the peak and turning point are the frequency of PM_{10}. But in 2013 and 2014, a noticeable decrease in dust abundance can be

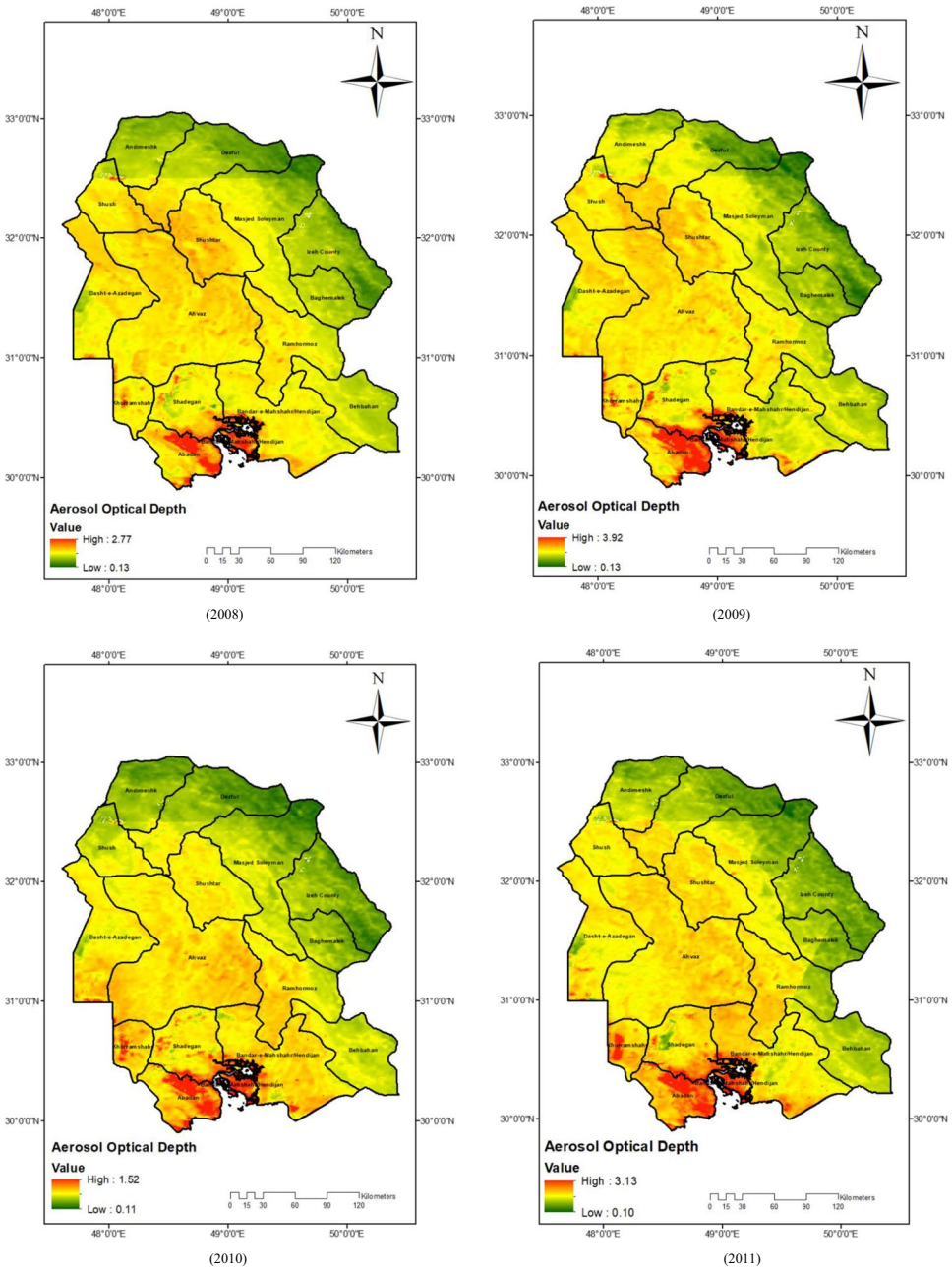


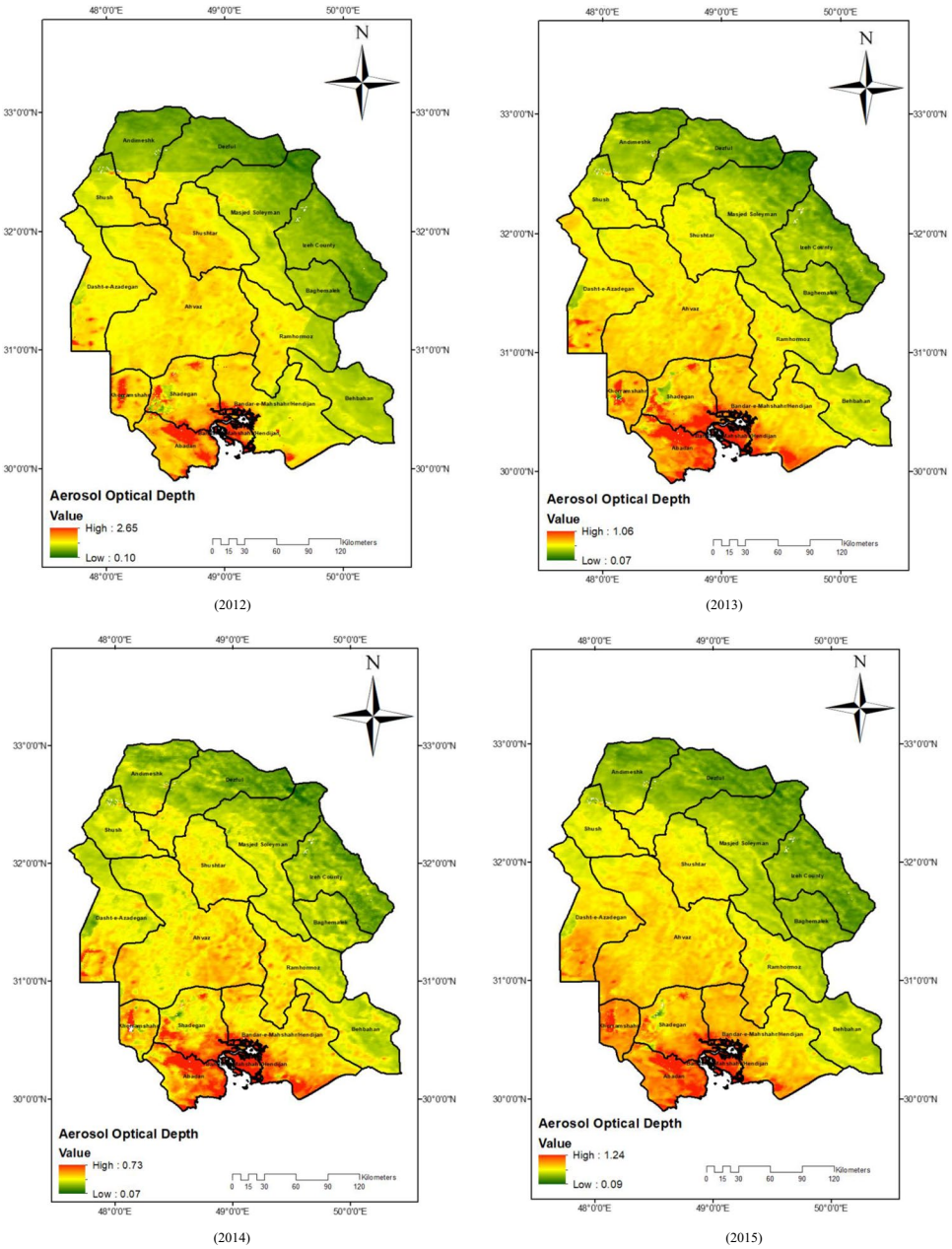
Fig. 4 Spatial distribution of aerosol optical depth (AOD) in the period of 2008–2018 at the study area

seen. Examination of temporal changes in monthly scale in synoptic stations of Khuzestan province showed that in June and July, more dust storm events occurred than other months of the year.

Relationship between AOD and meteorological parameters with particulate matter (PM_{10})

The levels and concentrations of pollutants are affected by meteorological parameters such as wind speed and direction,

Fig. 4 (continued)



precipitation (amount and period), air temperature, and relative humidity (Bhaskar et al. 2008; Farsani et al. 2018; Kliengchuay et al. 2018). Therefore, the effect of the meteorological parameters such as temperature, relative humidity, wind speed, and precipitation on the concentration of PM_{10} within a certain period was investigated in this study. The spatial variations of the relationships between the annual average PM_{10}, the annual average temperature (AAT), the annual average humidity ((AAH), the annual average wind speed (AAWS), and the annual average sum-precipitation (AAP) were assessed using the GWR model and OLS method. The results revealed the strong and stable correlation of PM_{10} with meteorological parameters.

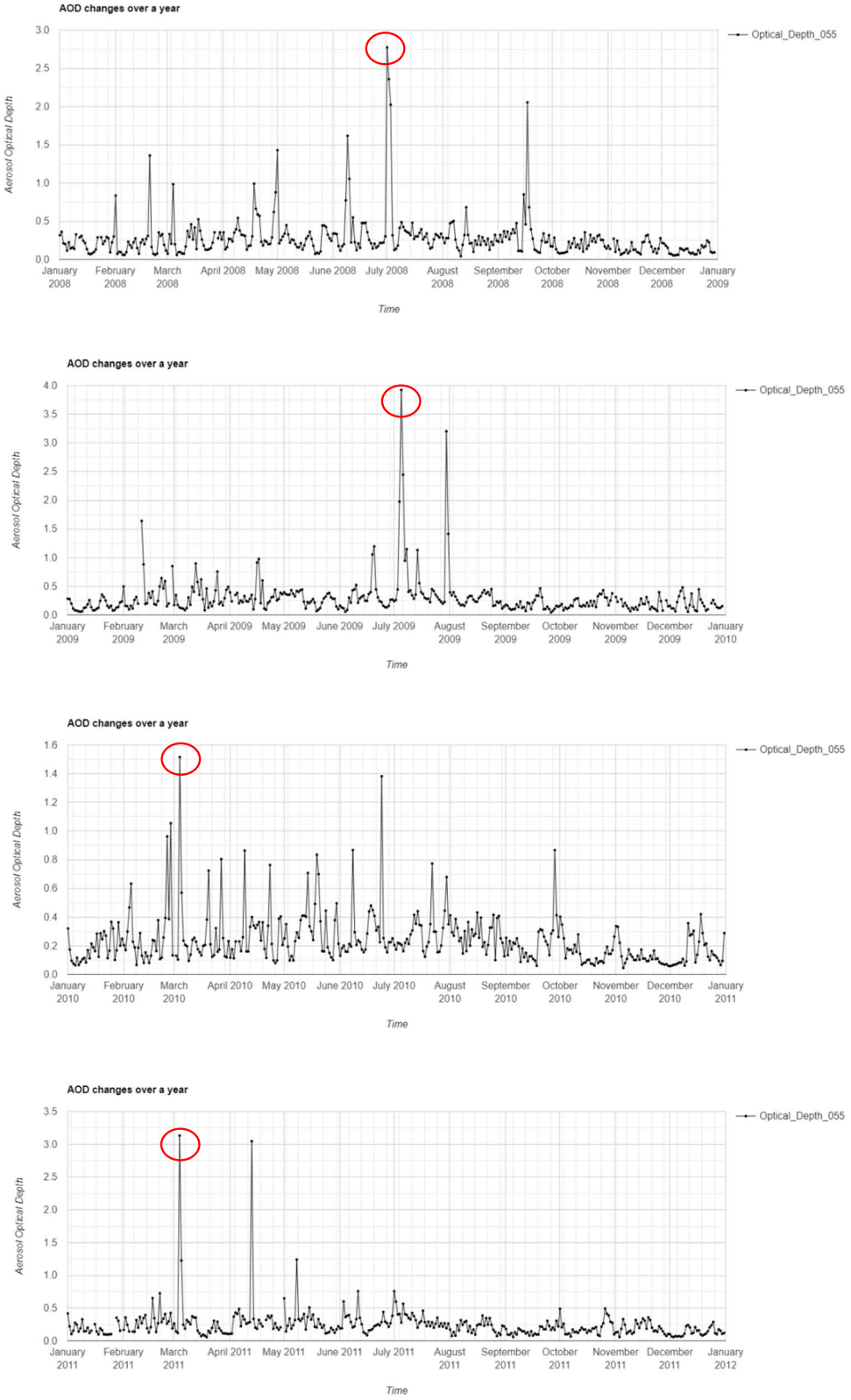


Fig. 5 Monthly change trends in the daily mean MODIS MAIAC AOD in the Khuzestan province for the period 2008–2018

Fig. 5 (continued)

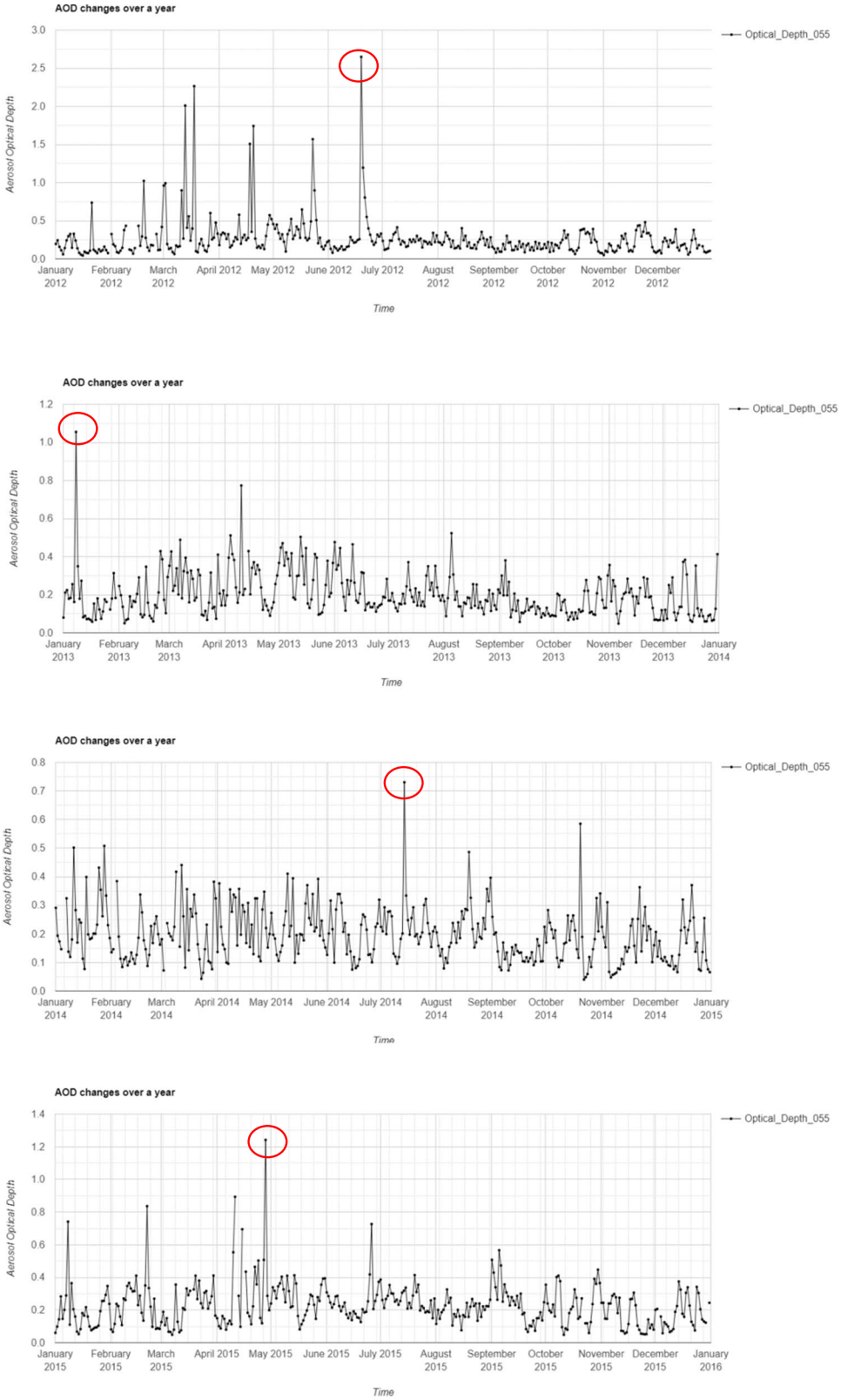
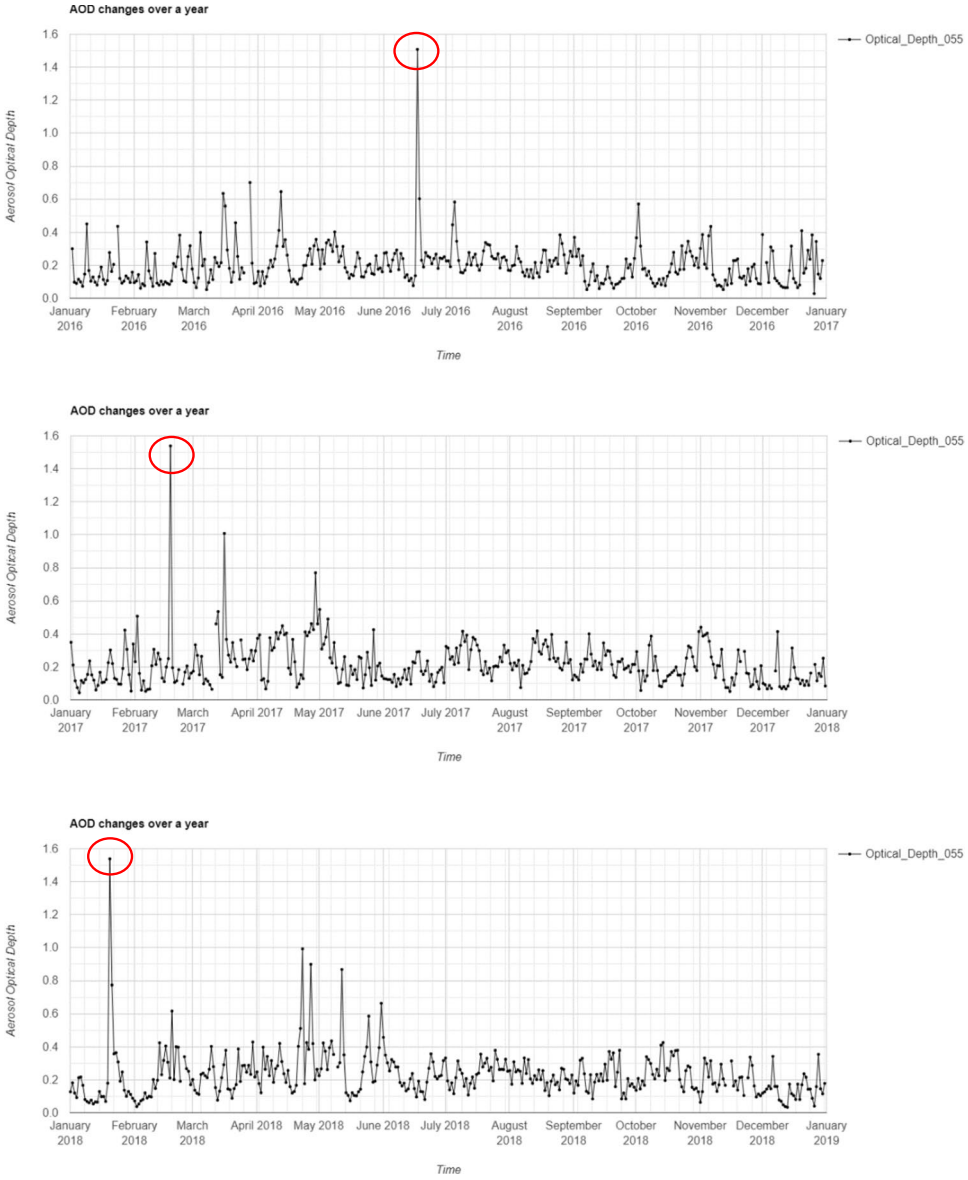


Fig. 5 (continued)



Statistical analyses related to particulate matter, meteorological parameters, and aerosol optical depth in 26 stations of Khuzestan province for each year in each of the 26 stations were examined separately. In this section, due to the limitation in the number of pages of the manuscript, only the annual average of the parameters mentioned above, related to all the stations of the study area during the years 2008 to 2018, is given in Table 1. Examination of the annual average of PM_{10}, and AOD showed that in 2008 and 2009, the peak of these parameters was in the whole study area (Table 1).

Examination of the results of the Pearson correlation coefficient showed that there is a very strong, significant, and positive relationship between PM_{10} and AOD index in the whole study period. The high correlation between these two parameters occurred almost all the years studied (Table 2). Also, the results of the Pearson correlation coefficient showed that there is a strong, significant, and positive correlation between PM_{10} with temperature and wind speed parameters. At the same time, there is a strong, powerful, and negative relationship between PM_{10} and precipitation parameters (Table 2). The increase in particulate matter concentrations in 2008 and 2009 could be due to dust emissions from strong winds, a decrease in relative humidity and sum precipitation, and a relative increase in temperature (Table 1). According to Javadian et al. (2019), dust storms in Iran are significantly caused by drought in Iraq. Similarly, dramatic desiccation of Iraq wetlands has contributed to increasing autumn dust events in southwest Iran (Javadian et al. 2019).

Table 1 Annual average PM concentration, AOD, and meteorological parameters comparison from 2008 to 2018 overall Khuzestan province

Year (overall)	AAT	AAH	AAWS	AAP	PM_{10}	AOD
2008	27.73	34.47	2.99	0.15	615.51	0.47
2009	26.12	39.22	2.71	0.30	448.72	0.49
2010	27.23	38.48	2.57	0.18	331.92	0.41
2011	25.79	38.72	2.76	0.30	476.39	0.43
2012	26.22	38.96	2.64	0.35	411.56	0.43
2013	25.69	41.33	2.66	0.25	366.91	0.39
2014	26.19	43.26	2.47	0.31	241.21	0.38
2015	26.81	42.04	2.57	0.34	517.12	0.39
2016	26.39	39.28	2.48	0.27	252.37	0.41
2017	26.24	39.55	2.53	0.66	334.33	0.46
2018	26.73	42.67	2.61	0.73	492.66	0.44

Comparison of LR, MLR, OLS, and GWR models for prediction of PM_{10}

After examining more than 300 pre-tests of the OLS model for 11 years for all stations in the study area, important meteorological factors affecting the concentration of particulate matter were identified. Then, a suitable platform was provided to implement the weighted geographical regression model in the study area. Table 3 summarizes the accuracy parameters of the fitted LR, MLR, GWR, and OLS models. The overall mean adjusted $R^2 = 0.89$ (GWR model) is greater than the overall mean adjusted $R^2 = 0.84$, 0.86, 0.85 LR, MLR, and OLS models, respectively. This section showed that among all the studied models, the GWR model has the highest accuracy in predicting the concentration of particulate matter (PM_{10}) in all stations of the Khuzestan province. It corroborates the supremacy of the GWR model over the OLS model in simulating PM_{10} concentrations. The results correspond to those from previous studies of GWR models (Hu et al. 2013; Zou et al. 2016; Xiao et al. 2018). The GWR result for 2009 and 2015 was the most accurate among the GWR results for the 11 years of study, with the highest adjusted R^2 (= 0.94, 0.95) and the low RMSE (= 27.40, 45.48 μg/m^3). Regarding the OLS results, the model with the highest adjusted R^2 (= 0.93) corresponds to 2009 and 2015. Also, the investigation of indicators such as MAE, root mean-squared errors (RMSE), Akaike's information criterion (AICc), adjusted coefficient of determination (R^2), normal (Z) scores, and Moran's I of the model residuals, to evaluate the accuracy of the studied models, was evidence of high accuracy and excellent performance of the GWR model in predicting the amount of particulate matter in the study area.

Table 2 Pearson correlation between PM_{10} concentration, AOD, and meteorological parameters comparison from 2008 to 2018 overall Khuzestan province

Variable/Year	AOD	T	RH	WS	p
PM_{10}/2008	0.96**	0.52	0.16	0.29	−0.62**
PM_{10}/2009	0.92**	0.18	−0.01	0.32	−0.69**
PM_{10}/2010	0.84**	0.34	0.22	0.19	−0.73**
PM_{10}/2011	0.85**	0.31	0.06	0.30	−0.67**
PM_{10}/2012	0.95**	0.26	0.36	0.39	−0.58*
PM_{10}/2013	0.95**	0.21	0.36	0.46	−0.73**
PM_{10}/2014	0.89**	0.28	0.19	0.28	−0.62*
PM_{10}/2015	0.96**	0.15	0.45	0.38	−0.56*
PM_{10}/2016	0.96**	0.27	0.20	0.70**	−0.48
PM_{10}/2017	0.95**	0.20	0.39	0.62*	0.35
PM_{10}/2018	0.94**	0.76**	−0.11	0.46	0.08

Table 4 shows the results of the leave-one-station-out cross-validation for different models. Results of this section also showed that the GWR was able to predict the values of PM_{10} in the study area and has better performance than the other three models, LR, MLR, and OLS. The overall mean $RMSE_{cv}$ and MAE_{cv} of the GWR model are 44.91 μg/m^3 and 35.98 μg/m^3, respectively, while those from the LR model are 56.59 μg/m^3, 45.06 μg/m^3, MLR model is 51.77 μg/m^3, and 39.34 μg/m^3 and OLS model are 52.21 μg/m^3 and 42.12 μg/m^3.

Comparison of observed vs. predicted PM_{10} concentrations from GWR model

Figure 6 shows the comparison between the amount of PM_{10} measured at air quality monitoring stations versus the amount of PM_{10} predicted by the GWR model during the studied time in overall stations of Khuzestan province. In general, it can be said that in all stations, there is a perfect relationship and perfect agreement between the values of PM_{10} measured with the predicted values of the GWR model in the study period. The results of this section also confirm the efficiency of the GWR model in predicting the concentration of PM_{10} in the overall Khuzestan province.

Table 3 Accuracy of utilized models: comparison between different models for predicted PM_{10} concentrations, expressed as R^2 coefficient, adjusted-R^2, RMSE, MAE, and AICc

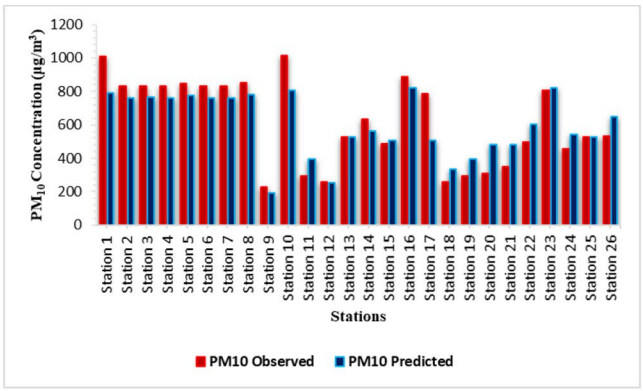
Statistical model	LR	MLR	OLS	GWR
Year	Accuracy indicators	Accuracy indicators	Accuracy indicators	Accuracy indicators
2008	$R^2 = 0.91$ Adjusted-$R^2 = 0.90$	$R^2 = 0.94$ Adjusted-$R^2 = 0.92$	RMSE = 69.77 MAE = 57.20 AICc = 197.56 $R^2 = 0.92$ Adjusted-$R^2 = 0.90$	RMSE = 50.17 MAE = 40.28 AICc = 186.61 $R^2 = 0.96$ Adjusted-$R^2 = 0.93$
2009	$R^2 = 0.85$ Adjusted-$R^2 = 0.84$	$R^2 = 0.97$ Adjusted-$R^2 = 0.95$	RMSE = 32.95 MAE = 25.13 AICc = 164.39 $R^2 = 0.94$ Adjusted-$R^2 = 0.93$	RMSE = 27.40 MAE = 20.15 AICc = 159.31 $R^2 = 0.96$ Adjusted-$R^2 = 0.94$
2010	$R^2 = 0.71$ Adjusted-$R^2 = 0.68$	$R^2 = 0.87$ Adjusted-$R^2 = 0.80$	RMSE = 59.90 MAE = 47.86 AICc = 185.54 $R^2 = 0.71$ Adjusted-$R^2 = 0.66$	RMSE = 52.98 MAE = 43.98 AICc = 177.36 $R^2 = 0.77$ Adjusted-$R^2 = 0.76$
2011	$R^2 = 0.73$ Adjusted-$R^2 = 0.71$	$R^2 = 0.78$ Adjusted-$R^2 = 0.66$	RMSE = 109.75 MAE = 94.71 AICc = 196.16 $R^2 = 0.72$ Adjusted-$R^2 = 0.70$	RMSE = 105.25 MAE = 89.87 AICc = 191.70 $R^2 = 0.75$ Adjusted-$R^2 = 0.74$
2012	$R^2 = 0.91$ Adjusted-$R^2 = 0.90$	$R^2 = 0.94$ Adjusted-$R^2 = 0.90$	RMSE = 46.91 MAE = 39.32 AICc = 166.20 $R^2 = 0.91$ Adjusted-$R^2 = 0.90$	RMSE = 37.15 MAE = 29.91 AICc = 165.80 $R^2 = 0.95$ Adjusted-$R^2 = 0.93$
2013	$R^2 = 0.91$ Adjusted-$R^2 = 0.90$	$R^2 = 0.94$ Adjusted-$R^2 = 0.90$	RMSE = 35.41 MAE = 31.41 AICc = 158.16 $R^2 = 0.91$ Adjusted-$R^2 = 0.90$	RMSE = 30.18 MAE = 25.04 AICc = 155.09 $R^2 = 0.94$ Adjusted-$R^2 = 0.92$
2014	$R^2 = 0.80$ Adjusted-$R^2 = 0.79$	$R^2 = 0.84$ Adjusted-$R^2 = 0.75$	RMSE = 37.04 MAE = 32.46 AICc = 162.37 $R^2 = 0.80$ Adjusted-$R^2 = 0.78$	RMSE = 34.79 MAE = 30.54 AICc = 159.12 $R^2 = 0.83$ Adjusted-$R^2 = 0.82$
2015	$R^2 = 0.94$ Adjusted-$R^2 = 0.93$	$R^2 = 0.95$ Adjusted-$R^2 = 0.93$	RMSE = 56.69 MAE = 38.39 AICc = 173.30 $R^2 = 0.94$ Adjusted-$R^2 = 0.93$	RMSE = 45.48 MAE = 33.62 AICc = 171.66 $R^2 = 0.96$ Adjusted-$R^2 = 0.95$
2016	$R^2 = 0.93$ Adjusted-$R^2 = 0.92$	$R^2 = 0.94$ Adjusted-$R^2 = 0.92$	RMSE = 23.11 MAE = 18.82 AICc = 156.92 $R^2 = 0.92$ Adjusted-$R^2 = 0.91$	RMSE = 20.71 MAE = 16.62 AICc = 148.79 $R^2 = 0.94$ Adjusted-$R^2 = 0.93$
2017	$R^2 = 0.90$ Adjusted-$R^2 = 0.89$	$R^2 = 0.91$ Adjusted-$R^2 = 0.90$	RMSE = 25.57 MAE = 19.78 AICc = 157.11 $R^2 = 0.91$ Adjusted-$R^2 = 0.89$	RMSE = 23.61 MAE = 16.65 AICc = 151.82 $R^2 = 0.93$ Adjusted-$R^2 = 0.92$
2018	$R^2 = 0.88$ Adjusted-$R^2 = 0.87$	$R^2 = 0.89$ Adjusted-$R^2 = 0.88$	RMSE = 78.14 MAE = 58.19 AICc = 191.02 $R^2 = 0.88$ Adjusted-$R^2 = 0.87$	RMSE = 67.04 MAE = 49.16 AICc = 185.33 $R^2 = 0.92$ Adjusted-$R^2 = 0.91$

Table 4 Results of Leave-one-station-out cross-validation for different models

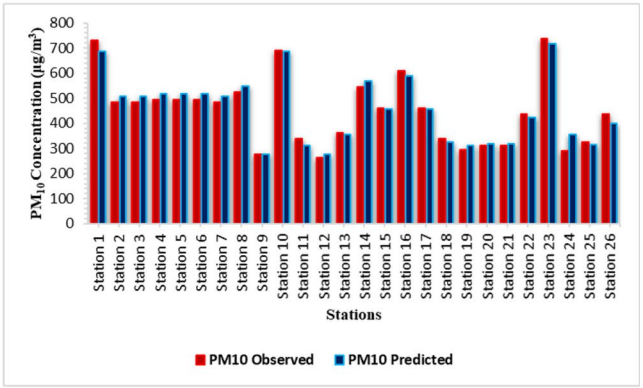
Model	Year										
	2008	2009	2010	2011	2012	2013	2014	2015	2016	2017	2018
LR	$RMSE_{CV}=82.29$ $MAE_{CV}=68.30$	$RMSE_{CV}=55.75$ $MAE_{CV}=49.39$	$RMSE_{CV}=57.98$ $MAE_{CV}=48.15$	$RMSE_{CV}=103.29$ $MAE_{CV}=84.03$	$RMSE_{CV}=50.31$ $MAE_{CV}=39.01$	$RMSE_{CV}=38.07$ $MAE_{CV}=31.60$	$RMSE_{CV}=37.10$ $MAE_{CV}=29.88$	$RMSE_{CV}=60.79$ $MAE_{CV}=39.71$	$RMSE_{CV}=25.86$ $MAE_{CV}=21.85$	$RMSE_{CV}=28.60$ $MAE_{CV}=22.38$	$RMSE_{CV}=82.49$ $MAE_{CV}=61.39$
MLR	$RMSE_{CV}=80.01$ $MAE_{CV}=65.48$	$RMSE_{CV}=37.78$ $MAE_{CV}=29.66$	$RMSE_{CV}=46.89$ $MAE_{CV}=35.16$	$RMSE_{CV}=98.52$ $MAE_{CV}=75.06$	$RMSE_{CV}=46.92$ $MAE_{CV}=35.02$	$RMSE_{CV}=35.08$ $MAE_{CV}=27.50$	$RMSE_{CV}=33.05$ $MAE_{CV}=25.99$	$RMSE_{CV}=56.72$ $MAE_{CV}=37.05$	$RMSE_{CV}=25.80$ $MAE_{CV}=21.48$	$RMSE_{CV}=27.37$ $MAE_{CV}=20.50$	$RMSE_{CV}=81.38$ $MAE_{CV}=59.88$
OLS	$RMSE_{CV}=69.68$ $MAE_{CV}=57.20$	$RMSE_{CV}=32.90$ $MAE_{CV}=25.13$	$RMSE_{CV}=59.84$ $MAE_{CV}=47.86$	$RMSE_{CV}=109.65$ $MAE_{CV}=94.71$	$RMSE_{CV}=46.87$ $MAE_{CV}=39.32$	$RMSE_{CV}=35.39$ $MAE_{CV}=31.41$	$RMSE_{CV}=37.02$ $MAE_{CV}=32.46$	$RMSE_{CV}=56.37$ $MAE_{CV}=38.39$	$RMSE_{CV}=23.09$ $MAE_{CV}=18.82$	$RMSE_{CV}=25.53$ $MAE_{CV}=19.78$	$RMSE_{CV}=78$ $MAE_{CV}=58.19$
GWR	$RMSE_{CV}=50.09$ $MAE_{CV}=40.28$	$RMSE_{CV}=27.36$ $MAE_{CV}=20.15$	$RMSE_{CV}=52.93$ $MAE_{CV}=43.98$	$RMSE_{CV}=105.14$ $MAE_{CV}=89.87$	$RMSE_{CV}=37.12$ $MAE_{CV}=29.91$	$RMSE_{CV}=30.16$ $MAE_{CV}=25.04$	$RMSE_{CV}=34.76$ $MAE_{CV}=30.54$	$RMSE_{CV}=45.31$ $MAE_{CV}=33.62$	$RMSE_{CV}=20.69$ $MAE_{CV}=16.62$	$RMSE_{CV}=23.55$ $MAE_{CV}=16.65$	$RMSE_{CV}=66.92$ $MAE_{CV}=49.16$

Conclusion

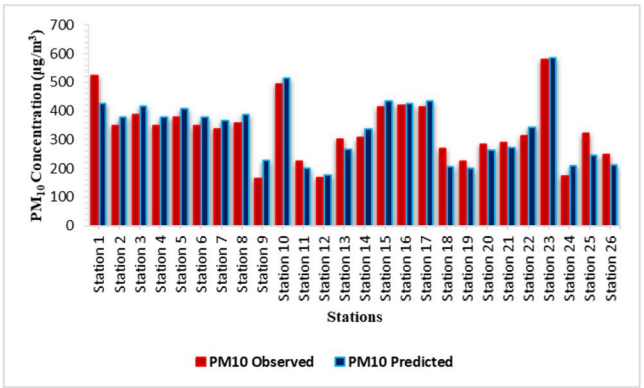
One of the main causes of air pollution in arid regions of the world, especially in Iran, is the occurrence of dust storms containing high concentrations of suspended particles with an aerodynamic diameter of less than 10 μm (PM_{10}). In recent years, due to reduced rainfall, successive droughts, vegetation degradation, wetland drying, intensification of wind erosion, and lack of long-term planning and investment to combat this phenomenon, the activity of sand and dust storms and, consequently, the concentration of particulate matter have increased over many desert areas of Iran, including Khuzestan province. Therefore, the purpose of this study is to investigate and monitor the concentration of particulate matter in 26 air quality monitoring stations throughout Khuzestan province of Iran along with meteorological data, aerosol optical depth, and their relationship using GIS services, statistical models, and remote sensing from January 2008 to December 2018. This research verified the MCD19A2 AOD product and studied the meteorological parameters in Khuzestan province. First, data measured by the air monitoring stations were used to verify the MCD19A2 product, where the high accuracy and reliability of MCD19A2 AOD were proved. It was also proved through the verifications that MCD19A2 can accurately demonstrate the aerosol distribution in the Khuzestan province of Iran. Analysis of mean annual MCD19A2 AOD data indicated that 2008 and 2009 were the most polluted in Khuzestan province out of the 11 years (2008–2018) of study. Then, the MCD19A2 data was used to analyze the meteorological parameters in this province using different regression models. Besides, the correlation between AOD and PM_{10} concentrations was studied to confirm the direct indication of MCD19A2 on air pollution. Results showed that AOD extracted from satellite products can be employed to predict PM_{10} mass concentrations in complex terrain such as Khuzestan province and provide a determination of PM_{10} spatial and temporal variability. The overall mean adjusted $R^2=0.89$ (GWR model) is greater than the overall mean adjusted $R^2=0.84$, 0.86, 0.85 LR, MLR, and OLS models, respectively. Among all the statistical models, the GWR performed better and had higher accuracy. These results and cross-validation suggested that the GWR model gives a more reliable way of predicting the spatial distribution of PM_{10} concentrations overall in Khuzestan province. Our model allows for the evaluation of short- and long-term human exposures. The findings of this study are beneficial and practical for the important and strategic province of Khuzestan, where the high concentration of particulate matter and severe dust storms along with severe shortage of water resources, reduced rainfall, drying of wetlands, and them becoming to internal sources of dust, are great problems and concerns.



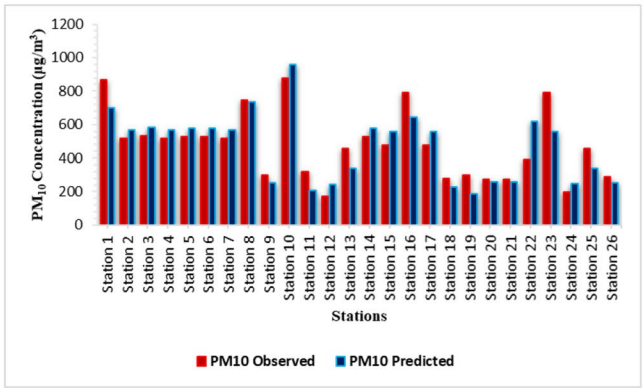
(2008)



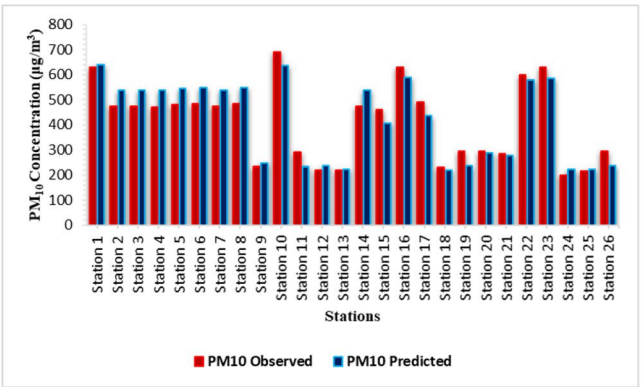
(2009)



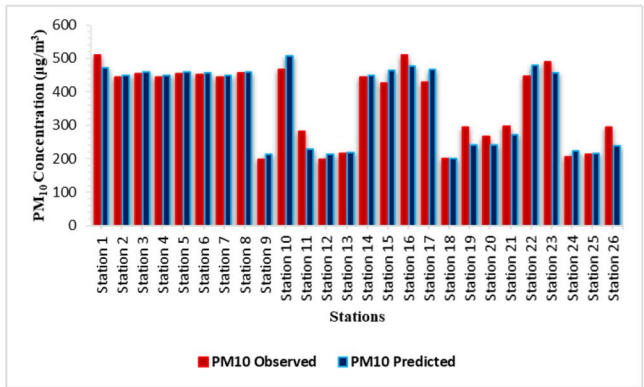
(2010)



(2011)

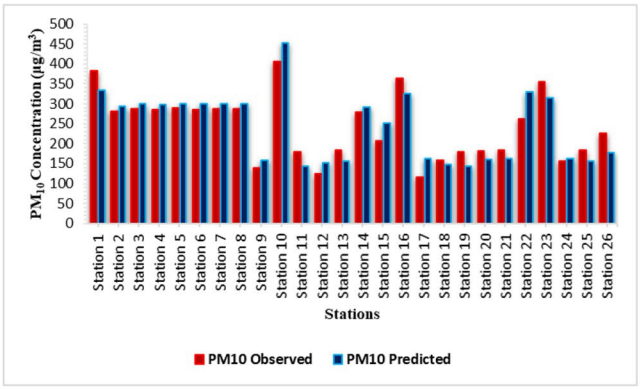


(2012)

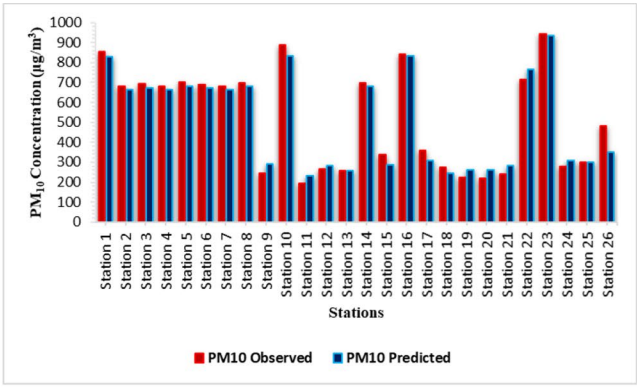


(2013)

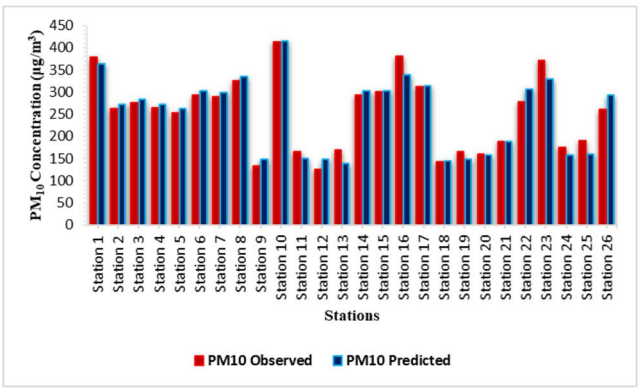
Fig. 6 Comparison of observed vs. predicted PM_{10} concentrations from GWR model in the different stations over Khuzestan province from **a** 2008 to **k** 2018



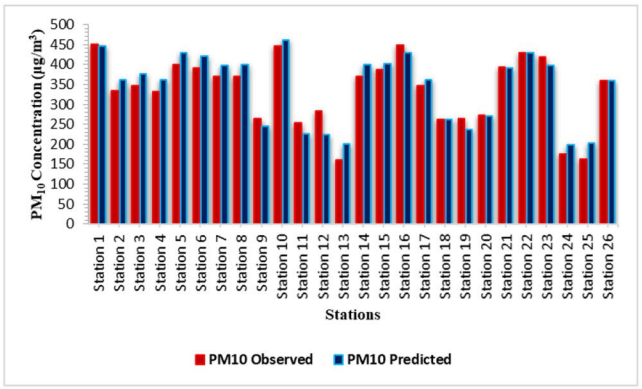
(2014)



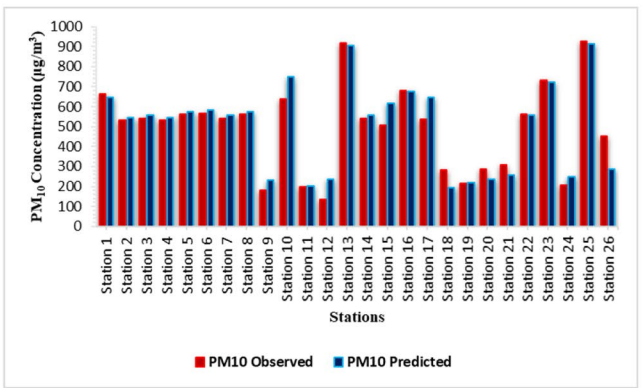
(2015)



(2016)



(2017)



(2018)

Fig. 6 (continued)

Data availability The data that support the findings of this study are available from the corresponding author upon reasonable request.

Declarations

Conflict of interest The authors declare no competing interests.

References

Abdollahi S, Madadi M, Ostad-Ali-Askari K (2021) Monitoring and investigating dust phenomenon on using remote sensing science, geographical information system and statistical methods. Appl Water Sci 11:111. https://doi.org/10.1007/s13201-02101419-z

Amani M, Ghorbanian A, Ahmadi SA, Kakooei M, Moghimi A, Mirmazloumi SM, Alizadeh Moghaddam SH, Mahdavi S, Ghahremanloo M, Parsian S, Wu Q, Brisco B (2020) Google Earth Engine cloud computing platform for remote sensing big data applications: a comprehensive review. IEEE J Sel Top Appl Earth Obs Remote Sens 13:5326–5350. https://doi.org/10.1109/JSTARS.2020.3021052

Ali MA, Assiri M, Dambul R (2017) Seasonal aerosol optical depth (AOD) variability using satellite data and its comparison over Saudi Arabia for the period 2002–2013. Aerosol Air Qual Res 17(5):1267–1280. https://doi.org/10.4209/aaqr.2016.11.0492

Ali G, Abbas S, Mueen Qamer F, Sing Wong M, Rasul G, Irteza SM, Shahzad N (2021) Environmental impacts of shifts in energy, emissions, and urban heat island during the COVID-19 lockdown across Pakistan. J Clean Prod 291(125806):1–12. https://doi.org/10.1016/j.jclepro.2021.125806

Al-Saadi J, Szykman J, Pierce RB, Kittaka C, Neil D, Chu DA, Remer L, Gumley L, Prins E, Weinstock L, MacDonald C, Wayland R, Dimmick F, Fishman J (2005) Improving national air quality forecasts with satellite aerosol observations. Bull Am Meteorol Soc 86:1249–1261. https://doi.org/10.1175/BAMS-86-9-1249

Azizi G, Miri M, Nabavi O (2012) Detection of Dust Phenomenon in Western Part of Iran. Iran J Arid Reg Geogr Stud 7(2):63–81

Balakrishnan K, Sankar S, Parikh J, Padmavathi R, Srividya K, Venugopal V, Prasad S, Pandey VL (2002) Daily average exposures to respirable particulate matter from combustion of biomass fuels in rural households of Southern India. Environ Health Perspect 110(11):1069–1075. https://doi.org/10.1289/ehp.021101069

Ballester F, Estarlich M, Iniguez C, Llop S, Ramon R, Esplugues A, Lacasana M, Rebagliato M (2010) Air pollution exposure during pregnancy and reduced birth size: a prospective birth cohort study in Valencia. Spain Environ Health 9(6):1–11. https://doi.org/10.1186/1476-069X-9-6

Bhaskar BV, Jeba Rajasekhar RV, Muthusubramanian P, Kesarkar AP (2008) Measurement and modelling of respirable particulate (PM_{10}) and lead pollution over Madurai, India. Air Qual Atmos Health 1:45–55. https://doi.org/10.1007/s11869-008-0004-0

Broomandi P, Dabir B, Bonakdarpour B, Rashidi Y (2018) Identification of the sources of dust storms in the city of Ahvaz by HYSPLIT. Pollution 3(2):341–348. https://doi.org/10.7508/PJ.2017.02.015

Chu DA, Kaufman YJ, Zibordi G, Chern JD, Mao J, Li C, Holben BN (2003) Global monitoring of air pollution over land from the Earth Observing System-Terra Moderate Resolution Imaging Spectrora-diometer (MODIS). J Geophys Res 108(D21):4661. https://doi.org/10.1029/2002JD003179

Chu Y, Liu Y, Li X, Liu Z, Lu H, Lu Y, Mao Z, Chen X, Li N, Ren M, Liu F, Tian L, Zhu Z, Xiang H (2017) A review on predicting ground $PM_{2.5}$ concentration using satellite aerosol optical depth. Atmos 7(129):1–25. https://doi.org/10.3390/atmos7100129

de Hoogh K, Héritier H, Stafoggia M, Künzli N, Kloog I (2018) Modelling daily $PM_{2.5}$ concentrations at high spatio-temporal resolution across Switzerland. Environ Pollut 233:1147–1154. https://doi.org/10.1016/j.envpol.2017.10.025

Di Q, Kloog I, Koutrakis P, Lyapustin A, Wang Y, Schwartz J (2016) Assessing $PM_{2.5}$ exposures with high spatiotemporal resolution across the continental United States. Environ Sci Technol 50:4712–4721. https://doi.org/10.1021/acs.est.5b06121

Dinoi A, Perrone MR, Burlizzi P (2010) Application of MODIS products for air quality studies over Southeastern Italy. Remote Sens 2(7):1767–1796. https://doi.org/10.3390/rs2071767

Dominici F, Peng RD, Bell ML, Pham L, McDermontt A, Zeger SL, Samet JM (2006) Fine particulate air pollution and hospital admission for cardiovascular and respiratory diseases. JAMA 295(10):1127–1134. https://doi.org/10.1001/jama.295.10.1127

Engel-Cox JA, Holloman CH, Coutant BW, Hoff RM (2004) Qualitative and quantitative evaluation of MODIS satellite sensor data for regional and urban scale air quality. Atmos Environ 38(16):2495–2509. https://doi.org/10.1016/j.atmosenv.2004.01.039

Environment in Iraq: UNEP Progress Report 2003 Retrieved from Switzerland

Faridi S, Shamsipour M, Krzyzanowski M, Künzli N, Amini H, Azimi F, Malkawi M, Momeniha F, Gholampour A, Hassanvand MS, Naddafi K (2018) Long-term trends and health impact of PM2.5 and O3 in Tehran, Iran, 2006–2015. Environ Int 114:37–49. https://doi.org/10.1016/j.envint.2018.02.026

Farsani MH, Shirmardi M, Alavi N, Maleki H, Sorooshian A, Babaei A, Asgharnia H, Bagherian Marzouni M, Goudarzi G (2018) Evaluation of the relationship between PM_{10} concentrations and heavy metals during normal and dusty days in Ahvaz. Iran Aeolian Res 13:12–22. https://doi.org/10.1016/j.aeolia.2018.04.001

Fotheringham AS, Charlton ME, Brunsdon C (1998) Geographically weighted regression: a natural evolution of the expansion method for spatial data analysis. Environ Plan A 30(11):1905–1927

Fotheringham AS, Brunsdon C, Charlton M (2002) Geographically weighted regression: the analysis of spatially varying relationships. Wiley, New York

Ghotbi S, Sotoudeheian S, Arhami M (2016) Estimating urban ground-level PM10 using MODIS 3km AOD product and meteorological parameters from WRF model. Atmos Environ 141:333–346. https://doi.org/10.1016/j.atmosenv.2016.06.057

Gorelick N, Hancher M, Dixon M, Ilyushchenko S, Thau D, Moore R (2017) Google Earth Engine: planetary-scale geospatial analysis for everyone. Remote Sens Environ 202:18–27. https://doi.org/10.1016/j.rse.2017.06.031

Grgurić S, Križan J, Gašparac G, Antonić O, Špirić Z, Mamouri RE, Christodoulou A, Nisantzi A, Agapiou A, Themistocleous K, Fedra K, Panayiotou C, Hadjimitsis D (2014) Relationship between MODIS based aerosol optical depth and PM_{10} over Croatia. Cent Eur J Geosci 6(1):2–16. https://doi.org/10.2478/s13533-012-0135-6

Han Y, Wu Y, Wang T, Zhuang B, Li S, Zhao K (2015) Impacts of elevated-aerosol layer and aerosol type on the correlation of AOD and particulate matter with ground-based and satellite measurements in Nanjing, southeast China. Sci Total Environ 532:195–207. https://doi.org/10.1016/j.scitotenv.2015.05.136

Ha Trang N, Tripathi NK (2014) Spatial correlation analysis between particulate matter 10 (PM_{10}) hazard and respiratory diseases in Chiang Mai Province, Thailand. Int. Arch. Photogramm. Remote Sens. Spatial Inf Sci XL-8:185-191. https://doi.org/10.5194/isprsarchives-XL-8-185-2014

Hatzianastassiou N, Matsoukas C, Drakakis E, Stackhouse JPW, Koepke P, Fotiadi A, Pavlakis KG, Vardavas I (2007) The direct effect of aerosols on solar radiation based on satellite

observations, reanalysis datasets, and spectral aerosol optical properties from Global Aerosol Data Set (GADS). Atmos Chem Phys 7:2585–2599

Haywood JM, Ramaswamy V (1998) Global sensitivity studies of the direct radiative forcing due to anthropogenic sulfate and black carbon aerosols. J Geophys Res 103:6043–6058

Hird JN, DeLancey ER, McDermid GJ, Kariyeva J (2017) Google Earth Engine, open-access satellite data, and machine learning in support of large-area probabilistic wetland mapping. Remote Sens 9(12):1315. https://doi.org/10.3390/rs9121315

Hu X, Waller LA, Al-Hamdan MZ, Crosson WL, Estes MG Jr, Estes SM, Quattrochi DA, Sarnat JA, Liu Y (2013) Estimating ground-level $PM_{2.5}$ concentrations in the Southeastern U.S. using geographically weighted regression. Environ Res 121:1–10. https://doi.org/10.1016/j.envres.2012.11.003

Hu X, Waller LA, Lyapustin A, Wang Y, Al-Hamdan MZ, Crosson WL, Estes MG Jr, Estes SM, Quattrochi DA, Puttaswamyet SJ, Liu Y (2014) Estimating ground-level $PM_{2.5}$ concentrations in the Southeastern United States using MAIAC AOD retrievals and a two-stage model. Rem Sens Environ 140:220–232. https://doi.org/10.1016/j.rse.2013.08.032

Hurvich CM, Simonoff JS, Tsai CL (1998) Smoothing parameter selection in nonparametric regression using an improved Akaike information criterion. J R Stat Soc Series B Stat Methodol 60(2):271–293. https://doi.org/10.1111/1467-9868.00125

Javadian M, Behrangi A, Sorooshian A (2019) Impact of drought on dust storms: case study over Southwest Iran. Environ Res Lett 14(12):1–9. https://doi.org/10.1088/1748-9326/ab574e

Kamarul Zaman NAF, Kanniah KD, Kaskaoutis DG (2017) Estimating particulate matter using satellite based aerosol optical depth and meteorological variables in Malaysia. Atmos Res 193:142–162. https://doi.org/10.1016/j.atmosres.2017.04.019

Karagulian F, Temimi M, Ghebreyesus D, Weston M, Kumar Kondapalli N, Krishnan Valappil V, Aldababesh A, Lyapustin A, Chaouch N, Al Hammadi F, Al Abdooli A (2019) Analysis of a severe dust storm and its impact on air quality conditions using WRF-Chem modeling, satellite imagery, and ground observations. Air Qual Atmos Health 12:453–470. https://doi.org/10.1007/s11869-019-00674-z

Kliengchuay W, Cooper Meeyai A, Worakhunpiset S, Tantrakarnapa K (2018) Relationships between meteorological parameters and particulate matter in Mae Hong Son Province, Thailand. Int J Environ Res Public Health 15(12):2801. https://doi.org/10.3390/ijerph15122801

Kloog I, Nordio F, Coull BA, Schwartz J (2012) Incorporating local land use regression and satellite aerosol optical depth in a hybrid model of spatiotemporal PM2.5 exposures in the Mid-Atlantic states. Environ Sci Technol 46(21):11913–11921. https://doi.org/10.1021/es302673e

Koelemeijer RBA, Homan CD, Matthijsen J (2006) Comparison of spatial and temporal variations of aerosol optical thickness and particulate matter over Europe. Atmos Environ 40(27):5304–5315. https://doi.org/10.1016/j.atmosenv.2006.04.044

Kolhe AR, Pawar GV, Varpe SR, Kumar PP, Devara PCS, Aher GR (2016) Multi-year analysis of aerosol properties retrieved from the Ångström parameters for different spectral ranges over Pune. Aerosol Air Qual Res 16(12):3266–3280. https://doi.org/10.4209/aaqr.2016.06.0268

Lee M, Kloog I, Chudnovsky A, Lyapustin A, Wang Y, Melly S, Coull B, Koutrakis P, Schwartz J (2015) Spatiotemporal prediction of fine particulate matter using high resolution satellite images in the Southeastern US 2003–2011. J Expo Sci Environ Epidemiol 26(4):377–384. https://doi.org/10.1038/jes.2015.41

Liu Z, Liu Q, Lin HC, Schwartz CS, Lee YH, Wang T (2011) Three-dimensional variational assimilation of MODIS aerosol optical depth: implementation and application to a dust storm over East Asia. J Geophys Res Atmos 116(D23206):1–19. https://doi.org/10.1029/2011JD016159

Liou K-N (2002) An introduction to atmospheric radiation. Academic press

Lyapustin A, Wang Y, Korkin S, Huang D (2018) MODIS collection 6 MAIAC algorithm. Atmos Meas Tech 11:5741–5765. https://doi.org/10.5194/amt-11-5741-2018

Ma J, Zhang W, Luo L, Xu Y (2013) China Statistical Yearbook- 2013

Mirzaei M, Amanollahi J, Tzanis CG (2019) Evaluation of linear, non-linear, and hybrid models for predicting $PM_{2.5}$ based on a GTWR model and MODIS AOD data. Air Qual Atmos Health 12:1215–1224. https://doi.org/10.1007/s11869-019-00739-z

Misra A, Jayaraman A, Ganguly D (2015) Validation of version 5.1 MODIS aerosol optical depth (deep blue algorithm and dark target approach) over a semi-arid location in Western India. Aerosol Air Qual Res 15:252–262. https://doi.org/10.4209/aaqr.2014.01.0004

Mokhtari A, Tashayo B, Deilami K (2021) Implications of nonstationary effect on geographically weighted total least squares regression for PM2.5 estimation. Int J Environ Res Public Health 18(13):7115. https://doi.org/10.3390/ijerph18137115

Noori R, Hoshyaripour G, Ashrafi K, NadjarArrabi B (2010) Uncertainty analysis of developed ANN and ANFIS model in prediction of carbon monoxide daily concentration. Atmos Environ 44:476–482. https://doi.org/10.1016/j.atmosenv.2009.11.005

Noroozi A, Shoaei Z (2018) Identifying areas with dust generation potential in the South West of Iran, case study: Khuzestan province. Watershed Eng Manage 10(3):398–409

Papadimas CD, Hatzianastassiou N, Mihaloppoulos N, Kanakidou M, Katsoulis BD, Vardavas I (2008) Assessment of the MODIS collections C005 and C004 aerosol optical depth products over the Mediterranean basin. Atmos Chem Phys 9:2987–2999. https://doi.org/10.5194/acp-9-2987-2009

Pawar GV, Devara PCS, Aher GR (2015) Identification of aerosol types over an urban site based on air-mass trajectory classification. Atmos Res 164:142–155. https://doi.org/10.1016/j.atmosres.2015.04.022

Pope CA, Burnett RT, Thun MJ, Calle EE, Krewski D, Ito K, Thurston GD (2002) Lung cancer, cardiopulmonary mortality, and long-term exposure to fine particulate air pollution. J Am Med Assoc 287(9):1132–1141. https://doi.org/10.1001/jama.287.9.1132

Pope CA, Brook RD, Burnett RT, Dockery DW (2011a) How is cardiovascular disease mortality risk affected by duration and intensity of fine particulate matter exposure? An integration of the epidemiologic evidence. Air Qual Atmos Health 4:5–14. https://doi.org/10.1007/s11869-010-0082-7

Pope CA, Burnett RT, Turner MC, Cohen A, Krewski D, Jerrett M, Gapstur SM, Thun MJ (2011b) Lung cancer and cardiovascular disease mortality associated with particulate matter exposure from ambient air pollution and cigarette smoke:shape of the exposure–response relationships. Environ Health Perspect 119:1616–1621. https://doi.org/10.1289/ehp.1103639

Ramanathan V, Carmichael G (2008) Global and regional climate changes due to black carbon. Nat Geosci 1:221–227. https://doi.org/10.1038/ngeo156

Seo S, Kim J, Lee H, Jeong U, Kim W, Holben BN, Kim S-W, Song CH, Lim JH (2015) Estimation of PM_{10} concentrations over Seoul using multiple empirical models with AERONET and MODIS data collected during the DRAGON-Asia campaign. Atmos Chem Phys 15:319–334. https://doi.org/10.5194/acp-15-319-2015

Soleimany A, Grubliauskas R, Šerevičienė V (2021) Application of satellite data and GIS services for studying air pollutants in Lithuania (case study: Kaunas city). Air Qual Atmos Health 14:411–429. https://doi.org/10.1007/s11869-020-00946-z

Stafoggia M, Schwartz J, Badaloni C, Bellander T, Alessandrini E, Cattani G, de'Donato F, Gaeta A, Leone G, Lyapustin A, Sorek-Hamer M, de Hoogh K, Di Q, Forastiere F, Kloog I (2016)

Estimation of daily PM_{10} concentrations in Italy (2006–2012) using finely resolved satellite data, land use variables and meteorology. Environ Int 99:234–244. https://doi.org/10.1016/j.envint.2016.11.024

Stafoggia M, Bellander T, Bucci S, Davoli M, de'Hoogh K, de Donato F, Gariazzo C, Lyapustin A, Michelozzi P, Renzi M, Scortichini M, Shtein A, Viegi G, Kloog I, Schwartz J (2019) Estimation of daily PM_{10} and $PM_{2.5}$ concentrations in Italy, 2013–2015, using a spatiotemporal land-use random-forest model. Environ Int 124:170–179. https://doi.org/10.1016/j.envint.2019.01.016

Tian J, Chen D (2010) Spectral, spatial, and temporal sensitivity of correlating MODIS aerosol optical depth with ground-based fine particulate matter ($PM_{2.5}$) across southern Ontario. Can J Remote Sens 36:119–128. https://doi.org/10.5589/m10-033

Wang Z, Zhou Y, Zhao R, Wang N, Biswas A, Shi Z (2021) High-resolution prediction of the spatial distribution of PM2.5 concentrations in China using a long short-term memory model. J Clean Prod 297(126493):1–11. https://doi.org/10.1016/j.jclepro.2021.126493

Wei Q, Zhang L, Duan W, Zhen Z (2019) Global and geographically and temporally weighted regression models for modeling PM2.5 in Heilongjiang, China from 2015 to 2018. Int J Environ Res Public Health 16:5107. https://doi.org/10.3390/ijerph16245107

Wu L, Li N, Yang Y (2018) Prediction of air quality indicators for the Beijing-Tianjin-Hebei region. J Clean Prod 196:682–687. https://doi.org/10.1016/j.jclepro.2018.06.068

Xiao L, Lang Y, Christakos G (2018) High-resolution spatiotemporal mapping of PM2.5 concentrations at Mainland China using a combined BME-GWR technique. Atmos Environ 173(295):305. https://doi.org/10.1016/j.atmosenv.2017.10.062

Zhang L, Gove JH, Heath LS (2005) Spatial residual analysis of six modeling techniques. Ecol Model 186:154–177

Zhang L, Ma Z, Guo L (2009) An evaluation of spatial autocorrelation and heterogeneity in the residuals of six regression models. Forest Sci 55(6):533–548

Zou B, Pu Q, Bilal M, Weng Q, Zhai L, Nichol JE (2016) High-resolution satellite mapping of fine particulates based on geographically weighted regression. IEEE Geosci Remote Sens Lett 13:495–499

Publisher's note Springer Nature remains neutral with regard to jurisdictional claims in published maps and institutional affiliations.

Authors and Affiliations

Arezoo Soleimany[1] · Eisa Solgi[1] · Khosro Ashrafi[2] · Reza Jafari[3] · Raimondas Grubliauskas[4]

[1] Department of Environment, Faculty of Natural Resources and Environment, Malayer University, Malayer, Iran

[2] School of Environment, College of Engineering, University of Tehran, Tehran, Iran

[3] Department of Natural Resources, Isfahan University of Technology, Isfahan, Iran

[4] Department of Environment Protection and Water Engineering, Faculty of Environmental Engineering, Vilnius Gediminas Technical University, Vilnius, Lithuania